

Adaptive Prediction Horizon-Based Model Predictive Control for Aero Engine

Guangao Liang[1], Linfeng Gou[1,*] & Linjun Lu[1]

[1] School of Power and Energy, Northwestern Polytechnical University, Xi'an, China

Abstract

Aero-engines are fast dynamic, strongly nonlinear, and highly constrained systems, making it challenging to simultaneously ensure constraint safety, disturbance rejection, and computational efficiency under uncertain disturbances. Although event-triggered model predictive control (ETMPC) can reduce unnecessary online optimization, conventional ETMPC usually relies on a fixed prediction horizon and accurate model prediction, which may limit its control performance under model uncertainties and external disturbances. To address this problem, this paper proposes a robust ETMPC method with an adaptive prediction horizon for aero-engine control. The triggering condition is constructed using state prediction errors and disturbance prediction errors to avoid unnecessary model predictive control (MPC) optimization. Meanwhile, the prediction horizon is dynamically adjusted according to the state deviation and disturbance intensity, improving the prediction capability during transient processes. Furthermore, an extended state observer (ESO) is combined with tube-based model predictive control (Tube-MPC) constraint tightening to estimate and compensate uncertain disturbances while enhancing robust constraint protection. Simulation results show that the proposed method achieves stable aero-engine control under parameter perturbations and external disturbances. Compared with the fixed-horizon ETMPC, the rise time of the low-pressure compressor speed is reduced by 29.6%, and the disturbance peak is reduced by 88.1%. These results demonstrate that the proposed method improves both dynamic response and disturbance rejection performance, providing a feasible solution for real-time robust optimal control of aero-engines.

Keywords: Aero-engine, Model predictive control, Adaptive prediction horizon, Event-triggered control, Extended state observer.

1. Introduction

The overall performance of an aircraft is closely related to the performance of its propulsion system[1]. With the increasing control performance requirements of next-generation aero-propulsion systems, aero-engine controllers are developing toward higher precision, faster real-time response, and improved stability[2]. However, aero-engines exhibit pronounced nonlinear, strongly coupled, and time-varying characteristics. Their operation is also subject to multiple safety constraints, such as temperature, rotational speed, and surge margin, and is easily affected by model uncertainties and external disturbances[3,4]. Existing control methods mainly focus on stability-oriented control, but they still have limitations in multivariable coordination, multi-objective optimization, and constraint handling, making it difficult to meet the increasing performance requirements of aero-engine control systems[5]. In addition, when limit protection is activated, conventional control strategies usually prioritize system stability, which may adversely affect dynamic response and tracking performance[6].

To address this issue, advanced control techniques need to be introduced. Model predictive control (MPC) has become an attractive control strategy because of its ability to systematically handle multivariable constraints[7]. However, the MPC optimization problem must be solved online at each sampling instant, which increases the computational burden[8] and makes it difficult to satisfy the real-time requirements of aero-engine control systems. Event-triggered control, as an effective and well-established strategy, aims to achieve a better trade-off between control performance and computational resource savings[9]. At present, most ETMPC triggering conditions are derived mainly based on system stability or recursive feasibility[10]. Such methods can reduce the computational burden to some extent and help meet the requirements of fast-response dynamic systems[11].

However, practical aero-engines are usually subject to uncertain disturbances, and conventional ETMPC relies heavily on model accuracy, making it difficult to guarantee effective control performance[12]. Therefore, disturbance-observer-based MPC compensation structures have been developed[13], along with disturbance-observer-based fuzzy MPC schemes[14] and disturbance-compensation control structures specifically designed for aero-engines[15]. Although these methods can alleviate performance degradation and stability problems of MPC under uncertain disturbances to some extent, most of them still rely on fixed prediction horizons or periodic online optimization mechanisms. As a result, they do not fully achieve a balanced trade-off among disturbance rejection capability, constraint robustness, and computational resource consumption.

To improve the disturbance rejection capability of ETMPC and satisfy the stability requirements of aero-engine control systems, an ETMPC method with an adaptive prediction horizon is introduced in this paper to enhance control performance. Meanwhile, an ESO is employed to estimate uncertain disturbances in real time, and the estimated disturbance is incorporated into the ETMPC control law as a compensation term, thereby reducing the adverse effects of disturbances on the system.

In this paper, an adaptive prediction horizon mechanism is first introduced within the ETMPC framework. The prediction horizon is dynamically adjusted according to the state deviation and disturbance intensity, allowing the controller to increase the prediction length when the system deviation becomes large or the disturbance is intensified, thereby improving its ability to anticipate future state variations and constraint risks. On this basis, an ESO-based disturbance compensation structure is further incorporated to estimate model uncertainties and external disturbances online. The estimated disturbance is then used for control compensation and triggering-condition evaluation, reducing the influence of disturbances on prediction accuracy and control performance.

The main contributions of this paper are summarized as follows:

An adaptive prediction horizon mechanism is developed to adjust N_P online according to the state deviation, residual disturbance bound, and contraction factor.

A Tube-MPC with ESO based robust compensation structure is proposed, where ESO estimates and compensates equivalent disturbances, while Tube-MPC tightens constraints to enhance robustness.

An integrated ETMPC framework combining adaptive prediction horizon and disturbance compensation is established for aero-engine control under multiple constraints and uncertain disturbances.

The remainder of this paper is organized as follows. Section 2 first develops an event-triggered model predictive controller based on a linear predictive model of the aero-engine. Then, an adaptive prediction horizon update method considering state deviation and disturbance effects is designed. Finally, an extended state observer is introduced to estimate multi-source uncertainties, and a compensation mechanism is employed to reduce the disturbance effects, followed by feasibility and stability analyses. Section 3 presents simulation validation and analysis of the proposed robust ETMPC framework with an adaptive prediction horizon. Section 4 provides the conclusions and discussion of this paper.

2. Methodology

The proposed control framework consists of three main components. First, an event-triggered MPC mechanism is designed to reduce unnecessary online optimization. Second, an adaptive prediction horizon strategy is introduced to improve prediction capability during transient operating conditions. Third, an ESO-based disturbance compensation structure is combined with Tube-MPC constraint tightening to enhance robustness against model uncertainties and external disturbances. The overall objective is to improve tracking performance, constraint satisfaction, disturbance rejection, and computational efficiency simultaneously.

2.1 Adaptive prediction horizon

2.1.1 Event triggered MPC

This paper takes a turbofan engine as the research object, as shown in Figure 1. Considering the strong nonlinearity and wide-envelope operating characteristics of aero-engines, a discrete-time linear parameter-varying (LPV) model is established. However, in practical controller design, aero-engines are inevitably subject to multiple sources of uncertainty, including linearization errors, external disturbances, and environmental noise. The system model can be expressed as

$$\begin{cases} \boldsymbol{x}(k+1) = \left(\boldsymbol{A}(\boldsymbol{\theta}) + \Delta\boldsymbol{A}\right)\boldsymbol{x}(k) + \left(\boldsymbol{B}(\boldsymbol{\theta}) + \Delta\boldsymbol{B}\right)\boldsymbol{u}(k) + \boldsymbol{E}_d\boldsymbol{d}(k) \\ \quad \boldsymbol{y}(k) = \boldsymbol{C}(\boldsymbol{\theta})\boldsymbol{x}(k) + \boldsymbol{v}(k) \end{cases} \tag{1}$$

where $\boldsymbol{A}(\boldsymbol{\theta})$, $\boldsymbol{B}(\boldsymbol{\theta})$ and $\boldsymbol{C}(\boldsymbol{\theta})$ are coefficient matrices dependent on the scheduling parameter $\boldsymbol{\theta}$. $\boldsymbol{x}(k)$ denotes the state vector, $\boldsymbol{y}(k)$ denotes the output vector, $\boldsymbol{u}(k)$ denotes the control input, and $k$is the sampling instant. $\Delta\boldsymbol{A}$ and $\Delta\boldsymbol{B}$ represent the uncertainty perturbations of the system matrix and input matrix, respectively. In addition, $\boldsymbol{d}(k)$ denotes the uncertain external scalar disturbance, and $\boldsymbol{v}(k)$ denotes the measurement noise. $\boldsymbol{E}_d$ is the disturbance input matrix

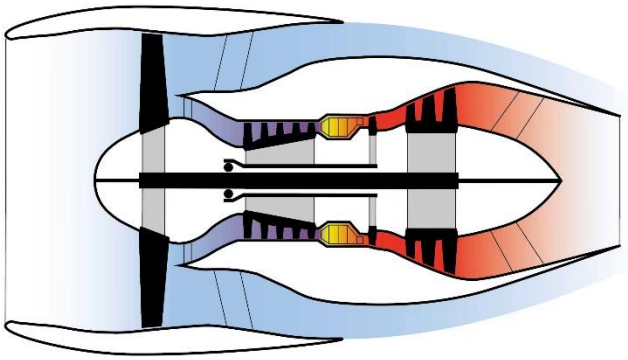


Figure 1. turbofan engine

Based on the above model, the event-triggering mechanism of ETMPC is investigated. The ETMPC design is still based on the aero-engine model with uncertain disturbances given in Eq. (1). The state prediction error and disturbance prediction error are measured using the P-norm, as expressed in Eq. (1) and Eq. (2):

$$\begin{aligned} \boldsymbol{e}_x(k) &= \boldsymbol{x}(k) - \hat{\boldsymbol{x}}(k|k_p) \\ \boldsymbol{E}_x(k) &= \left\|\boldsymbol{e}_x(k)\right\|_{\boldsymbol{P}} \end{aligned} \tag{1}$$

$$\begin{aligned} \boldsymbol{e}_d(k+m) &= \hat{\boldsymbol{d}}\left(k+m|k\right) - \hat{\boldsymbol{d}}\left(k+m|k_p\right) \\ \boldsymbol{E}_w(k) &= \sum_{s=0}^{N_r(k)-1} \left\|\boldsymbol{E}_d\boldsymbol{e}_w(k+s)\right\|_{\boldsymbol{P}} \end{aligned} \tag{2}$$

where $\boldsymbol{x}(k)$ in Eq. (1) denotes the actual state, $\hat{\boldsymbol{x}}(k|k_p)$ represents the prediction of the current state obtained at the previous triggering instant, and $k_p$denotes the previous triggering instant. Moreover,

$\hat{\boldsymbol{d}}(k+m|k)$ is the disturbance prediction made at time k, while $\hat{\boldsymbol{d}}(k+m|k_p)$ is the disturbance prediction obtained at time k_p. The remaining prediction horizon is defined as

$$N_r(k) = N_p - (k - k_p) \tag{3}$$

Accordingly, the comprehensive triggering index is formulated as

$$\begin{aligned} \Gamma_k &= c_x \boldsymbol{E}_x(k) + c_w \boldsymbol{E}_w(k) \\ &= c_x \left\| \boldsymbol{x}(k|k) - \boldsymbol{x}(k|k_p) \right\|_{\boldsymbol{P}} + c_w \sum_{s=0}^{N_r(k)-1} L_p^s \left\| \boldsymbol{E}_d \boldsymbol{e}_w(k+s) \right\|_{\boldsymbol{P}} \end{aligned} \tag{4}$$

In Eq. (4), L_p^s is the weighting term associated with the Lipschitz amplification factor, c_x is the weight of the state prediction error, and c_w is the weight of the disturbance prediction error. A larger value of Γ_k indicates that the control sequence obtained from the previous MPC optimization becomes less reliable.

2.1.2 Event triggered Adaptive prediction horizion

Based on the ETMPC framework, an adaptive prediction horizon is designed in this paper. At time k, the state deviation $\boldsymbol{e}_k(k) = \boldsymbol{x}(k) - \boldsymbol{x}_r$, input deviation $\boldsymbol{v}_k(k) = \boldsymbol{u}(k) - \boldsymbol{u}_r$, disturbance deviation $\boldsymbol{w}_k(k) = \boldsymbol{d}(k) - \boldsymbol{d}_r$, and output deviation $\tilde{\boldsymbol{y}}_k$, $\boldsymbol{x}_r$ denotes the desired state. The MPC prediction model in deviation form is given by

$$\begin{cases} \boldsymbol{e}_k(k+i+1|k) = \boldsymbol{A}(\boldsymbol{\theta}) \boldsymbol{e}_k(k+i|k) + \boldsymbol{B}(\boldsymbol{\theta}) \boldsymbol{v}_k(k+i|k) + \boldsymbol{E}_d \boldsymbol{w}_k(k+i|k) \\ \tilde{\boldsymbol{y}}(k+i|k) = \boldsymbol{C}(\boldsymbol{\theta}) \boldsymbol{e}_k(k+i|k) \end{cases} \tag{5}$$

For standard MPC stability, the terminal predicted state is usually required to enter the terminal region, namely:

$$\boldsymbol{e}_k(k+N_p|k) \in \chi_f \tag{6}$$

where:

$$\chi_f = \{ \boldsymbol{e}_k : \left\| \boldsymbol{e}_k(k+N_P|k) \right\|_{\boldsymbol{P}} \le \varepsilon_{\boldsymbol{x}} \} \tag{7}$$

To ensure that the MPC predicted closed-loop system remains contractive while the residual disturbance is bounded, the following conditions are imposed:

$$\begin{aligned} &\left\| \boldsymbol{e}_k(k+i+1|k) \right\|_{\boldsymbol{P}} \le \rho \left\| \boldsymbol{e}_k(k+i|k) \right\|_{\boldsymbol{P}} + \left\| \boldsymbol{E}_d \boldsymbol{w}_k(k+i|k) \right\|_{\boldsymbol{P}} \\ &\left\| \boldsymbol{w}_k(k+i|k) \right\| \le \bar{\boldsymbol{w}}_k \end{aligned} \tag{8}$$

where $0 < \rho < 1$ denotes the convergence rate of the predicted closed-loop system, and $\bar{\boldsymbol{w}}_k$ represents the upper bound of the residual disturbance. Combining the above conditions with the terminal constraint, the adaptive prediction horizon can be further derived.

$$\left\| \boldsymbol{e}_k(k+N_p|k) \right\|_{\boldsymbol{P}} \le \rho^{N_p} \left\| \boldsymbol{e}_k(k|k) \right\|_{\boldsymbol{P}} + \sum_{j=0}^{N_p-1} \rho^j \left\| \boldsymbol{E}_d \right\|_{\boldsymbol{P}} \bar{\boldsymbol{w}}_k \le \varepsilon_{\boldsymbol{x}} \tag{9}$$

Let $\gamma = \dfrac{\left\| \boldsymbol{E}_d \right\|_{\boldsymbol{P}}}{1-\rho}$, Substituting this expression into Eq. (9) yields:

$$N_p \ge \frac{\ln\left(\dfrac{\varepsilon_{\boldsymbol{x}} - \gamma \bar{\boldsymbol{w}}_k}{\left\| \boldsymbol{x}(k|k) - \boldsymbol{x}_r \right\| - \gamma \bar{\boldsymbol{w}}_k} \right)}{\ln \rho} \tag{10}$$

Equation (10) indicates that when the aero-engine state exhibits a large deviation or when a strong disturbance occurs, a longer prediction horizon is required for MPC to anticipate future state variations and constraint risks in advance. In this paper, the single-step variation of the prediction horizon N_p is set to 2.

Equation (10) indicates that the required prediction horizon is directly related to the current state

deviation and residual disturbance bound. When the aero-engine operates in a rapid transient process, such as acceleration or disturbance rejection, the state deviation becomes larger and a longer prediction horizon is required to predict future constraint risks. In contrast, when the system approaches steady-state operation, the prediction horizon can be reduced to decrease the computational burden without significantly degrading control performance.

2.1.3 Feasibility and stability analysis

For the recursive feasibility of the adaptive prediction horizon, suppose that the current triggering instant is $k=k_p+s$, where k_p denotes the previous triggering instant. The prediction horizon at k_p is denoted by N_{p,k_p}, and the remaining prediction steps at the current instant are therefore given by $N_{r,k}=N_{p,k}-s$.To ensure that a feasible candidate control sequence can still be constructed based on the cached control sequence at the current instant, a new prediction horizon $N_{p,s}$ is defined. It is required that N_p has upper and lower bounds and satisfies:

$$N_{p,s}\geq N_{p,k}-\left(k-k_p\right) \tag{11}$$

The stability of the ETMPC with adaptive N_p is then analysed. It is assumed that all MPC problems with admissible prediction horizons use the same terminal weight matrix $\boldsymbol{P}$ and terminal set $\mathcal{X}$, and that the optimal cost function corresponding to each prediction horizon is bounded from above and below. Define the Lyapunov function as $\boldsymbol{V}_{N_p}\left(\boldsymbol{e}_k\right)=J^*_{N_p}\left(\boldsymbol{e}_k\right)$. Based on the stability property of the nominal MPC, one obtains:

$$\boldsymbol{V}_{N_p}\left(\boldsymbol{e}_k\left(k\right)\right)-\boldsymbol{V}_{N_p}\left(\boldsymbol{e}_k\left(k+1\right)\right)\leq \boldsymbol{e}_k^{\boldsymbol{T}}\left(k\right)\boldsymbol{Q}\boldsymbol{e}_k\left(k\right)+\boldsymbol{v}_k^{\boldsymbol{T}}\left(k\right)\boldsymbol{R}\boldsymbol{v}_k\left(k\right) \tag{12}$$

where $\boldsymbol{Q}$ is the state weighting matrix, $\boldsymbol{R}$ is the input weighting matrix.

For ETMPC, since the cached control sequence is continuously applied during non triggered intervals, there exists a deviation between the actual state and the predicted state. Meanwhile, the system is affected by bounded residual disturbances. Therefore, the descent condition can be relaxed as

$$\boldsymbol{V}_{N_p}\left(\boldsymbol{e}_k\left(k\right)\right)-\boldsymbol{V}_{N_p}\left(\boldsymbol{e}_k\left(k+1\right)\right)\leq \boldsymbol{e}_k^{\boldsymbol{T}}\left(k\right)\boldsymbol{Q}\boldsymbol{e}_k\left(k\right)+\boldsymbol{v}_k^{\boldsymbol{T}}\left(k\right)\boldsymbol{R}\boldsymbol{v}_k\left(k\right)+\boldsymbol{c}_{\Gamma}\Gamma_k^2+\boldsymbol{c}_{\eta}\bar{\eta}_k^2 \tag{13}$$

where $\bar{\eta}$ denotes the upper bound of the residual disturbance. Since the event-triggering mechanism guarantees $\Gamma_k\leq\Delta_k$ during non-triggered intervals, and $\Delta_k\leq\bar{\Delta}_k$, the effect of prediction deviation and residual disturbance can be bounded in the stability analysis.

where $\bar{\eta}$ denotes the upper bound of the residual disturbance. Since the event-triggering mechanism guarantees that $\Gamma_k\leq\Delta_k$ during non-triggered intervals, and $\Delta_k\leq\bar{\Delta}_k$, while the stage cost satisfies

$$\boldsymbol{e}_k^{\boldsymbol{T}}\left(k\right)\boldsymbol{Q}\boldsymbol{e}_k\left(k\right)+\boldsymbol{v}_k^{\boldsymbol{T}}\left(k\right)\boldsymbol{R}\boldsymbol{v}_k\left(k\right)\geq\alpha\left\|\boldsymbol{e}_k\left(k\right)\right\|^2 \tag{14}$$

one obtains

$$\boldsymbol{V}_{N_p}\left(\boldsymbol{e}_k\left(k\right)\right)-\boldsymbol{V}_{N_p}\left(\boldsymbol{e}_k\left(k+1\right)\right)\leq\alpha\left\|\boldsymbol{e}_k\left(k\right)\right\|^2+\boldsymbol{c}_{\Gamma}\bar{\Delta}_{\boldsymbol{k}}{}^2+\boldsymbol{c}_{\eta}\bar{\eta}_k^2 \tag{15}$$

Therefore, when

$$\left\|\boldsymbol{e}_k\left(k\right)\right\|^2\geq\frac{\boldsymbol{c}_{\Gamma}\bar{\Delta}_{\boldsymbol{k}}{}^2+\boldsymbol{c}_{\eta}\bar{\eta}_k^2}{\alpha},$$

the optimal value function strictly decreases. Combining the positive definiteness and boundedness of $\boldsymbol{V}_{N_p}\left(\boldsymbol{e}_k\left(k\right)\right)$, the closed-loop state eventually enters and remains within a bounded neighborhood determined jointly by the triggering threshold and the residual disturbance, namely

$$\limsup_{k\to\infty}\left\|\boldsymbol{e}_k\left(k\right)\right\|\leq\sqrt{\frac{\boldsymbol{c}_{\Gamma}\bar{\Delta}_{\boldsymbol{k}}{}^2+\boldsymbol{c}_{\eta}\bar{\eta}_k^2}{\alpha}} \tag{16}$$

Thus, the recursive feasibility and stability of the ETMPC with an adaptive prediction horizon are established.

2.2 ETMPC structure with ESO

2.2.1 Adaptive event-triggered model predictive control

For the system described by Eq. (1), the Tube-MPC optimization problem to be solved is formulated as follows:

$$\boldsymbol{u}^*(k+s|k)=\arg\min_{\boldsymbol{u}(k+s|k)} J\left(\hat{\boldsymbol{x}}(k+s|k),\hat{\boldsymbol{u}}(k+s|k)\right) \tag{17}$$

$$\begin{aligned} s.t. \quad & \hat{\boldsymbol{x}}(k|k)=\boldsymbol{x}(k) \\ & \hat{\boldsymbol{y}}(k+s|k)=\mathcal{Y} \\ & \hat{\boldsymbol{u}}(k+s|k)\in\mathcal{U}\ominus\boldsymbol{K}\Omega \\ & \Delta\hat{\boldsymbol{u}}(k+s|k)\in\mathcal{U}' \\ & \hat{\boldsymbol{x}}(k+N_p|k)\in\mathcal{X}\ominus\Omega \end{aligned} \tag{18}$$

where $\boldsymbol{P}$ is the terminal weighting matrix, $\hat{\boldsymbol{x}}$ denotes the predicted state, $\hat{\boldsymbol{y}}$ denotes the predicted output, and $\hat{\boldsymbol{u}}$ denotes the predicted input. The terminal set is defined as

$$\mathcal{X}=\{\boldsymbol{x}:\left(\hat{\boldsymbol{x}}\left(k+N_p|k\right)-\boldsymbol{x}_r\right)^T\boldsymbol{P}\left(\hat{\boldsymbol{x}}\left(k+N_p|k\right)-\boldsymbol{x}_r\right)\le\varepsilon_f^2\} \tag{19}$$

where ε_f is the terminal error radius. $\mathcal{Y}$, $\mathcal{U}$,and $\mathcal{U}'$ denote the output constraint set, input constraint set, and input rate constraint set, respectively. s is the current prediction step. The MPC control output is denoted by $\boldsymbol{u}_{MPC}(k)$, $\boldsymbol{K}$ is the feedback gain matrix, and Ω is the robust invariant set.

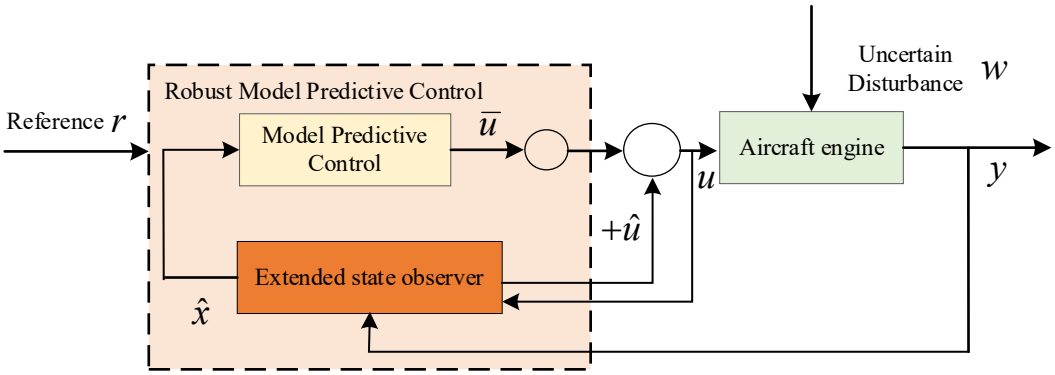


Figure 2. MPC Control Structure with ESO

Based on Eq.(1), an ESO-based disturbance-rejection offset-free MPC design is further developed. First, the uncertain disturbances are combined into a unified term $\boldsymbol{\Phi}$, yielding

$$\begin{cases} \boldsymbol{x}(k+1)=\boldsymbol{A}(\boldsymbol{\theta})\boldsymbol{x}(k)+\boldsymbol{B}(\boldsymbol{\theta})\boldsymbol{u}(k)+\boldsymbol{\Phi}(k) \\ \boldsymbol{y}(k)=\boldsymbol{C}(\boldsymbol{\theta})\boldsymbol{x}(k)+\boldsymbol{v}(k) \\ \boldsymbol{\Phi}(k)=\Delta\boldsymbol{A}\boldsymbol{x}(k)+\Delta\boldsymbol{B}\boldsymbol{u}(k)+\boldsymbol{E}_d\boldsymbol{d}(k) \end{cases} \tag{20}$$

In practical aero-engine control, model uncertainties, linearization errors, actuator deviations, and external disturbances may simultaneously affect the system dynamics. Instead of modeling each uncertainty source separately, these effects are combined into a lumped disturbance term $\boldsymbol{\Phi}$. This treatment simplifies the observer design and enables the disturbance compensation to be incorporated into the MPC framework.

The multi-source uncertain disturbances are uniformly treated as additive disturbances, and an ESO-based compensation structure is designed. First, the disturbance is defined as an extended state, $\boldsymbol{x}_E=\begin{bmatrix}\boldsymbol{x}(k)\\ \boldsymbol{\Phi}(k)\end{bmatrix}$. Based on the extended model, the LPV extended state observer is constructed as

$$\begin{aligned} \boldsymbol{x}_E(k+1) &= \boldsymbol{A}_E(\boldsymbol{\theta})\boldsymbol{x}_E(k) + \boldsymbol{B}_E(\boldsymbol{\theta})\boldsymbol{u}(k) + \boldsymbol{L}_E(\boldsymbol{y}(k) - \boldsymbol{y}_E(k)) \\ \boldsymbol{y}_E(k) &= \boldsymbol{C}_E(\boldsymbol{\theta})\boldsymbol{x}_E(k) \end{aligned} \tag{21}$$

where $\boldsymbol{A}_E(\boldsymbol{\theta}) = \begin{bmatrix} \boldsymbol{A}(\boldsymbol{\theta}) & \boldsymbol{E}_d \\ 0 & \boldsymbol{I} \end{bmatrix}$, $\boldsymbol{B}_E(\boldsymbol{\theta}) = \begin{bmatrix} \boldsymbol{B}(\boldsymbol{\theta}) \\ 0 \end{bmatrix}$, $\boldsymbol{C}_E(\boldsymbol{\theta}) = \begin{bmatrix} \boldsymbol{C}(\boldsymbol{\theta}) & 0 \end{bmatrix}$, $\boldsymbol{L}_E$ is the ESO gain matrix, $\boldsymbol{x}_E$ denotes the estimated extended state, and $\boldsymbol{y}_E$ denotes the estimated output. The observer gain $\boldsymbol{L}_E$ is obtained by solving the discrete algebraic Riccati equation.

Considering that the actual disturbance $\boldsymbol{\Phi}$ is not constant, namely $\boldsymbol{\Phi}(k) \neq \boldsymbol{\Phi}(k+1)$, the compensation input calculated by a conventional ESO feedback compensation strategy may not effectively cancel the next-step disturbance $\boldsymbol{\Phi}(k+1)$. Therefore, a Fourier-transform-based approach is introduced in this paper. The currently estimated disturbance is first transformed into the frequency domain, and then a first-order linear extrapolation method is used to predict the disturbance at the next sampling instant. In this way, the ESO-based compensation can better match the estimated disturbance $\hat{\boldsymbol{\Phi}}(k+1)$.

Using Eq. (21), the disturbance estimate $\hat{\boldsymbol{\Phi}}(k)$ can be obtained, and the corresponding compensation input and total control input are calculated as

$$\begin{aligned} \boldsymbol{u}_{ESO}(k) &= -\boldsymbol{B}^{-1}(\boldsymbol{\theta})\hat{\boldsymbol{\Phi}}(k) \\ \boldsymbol{u}_{total}(k) &= \boldsymbol{u}_{MPC}(k) + \boldsymbol{u}_{ESO}(k) \end{aligned} \tag{22}$$

where $\boldsymbol{u}_{ESO}(k)$ denotes the compensation input generated from the ESO-based disturbance estimate, and $\boldsymbol{u}_{total}(k)$ represents the total control input applied to the system. The compensation input is used as a feedforward term to reduce the influence of the estimated lumped disturbance. Therefore, the MPC component mainly handles tracking and constraint satisfaction, while the ESO-based compensation component improves disturbance rejection performance.

2.2.2 Feasibility and stability analysis

The stability of the proposed ESO-MPC controller is analysed in this subsection. Substituting the control input into the system model yields

$$\boldsymbol{x}(k+1) = \boldsymbol{A}(\boldsymbol{\theta})\boldsymbol{x}(k) + \boldsymbol{B}(\boldsymbol{\theta})(\boldsymbol{u}_{MPC} + \boldsymbol{u}_{ESO}) + \boldsymbol{\Phi}(k) \tag{23}$$

Let

$$\upsilon(k) = \boldsymbol{\Phi}(k) - \hat{\boldsymbol{\Phi}}(k) = \boldsymbol{e}_{\boldsymbol{\Phi}}(k).$$

When the disturbance estimation error is bounded, the following inequality holds:

$$\left\|\upsilon(k)\right\| \leq \left\|\boldsymbol{e}_{\boldsymbol{\Phi}}(k)\right\| \leq \left\|\bar{\upsilon}_{ESO}(k)\right\| \tag{24}$$

where $\bar{\upsilon}_{ESO}(k)$ denotes the disturbance upper bound determined by the estimation accuracy of the ESO. Therefore, under the ESO-MPC closed-loop condition, the actual system can be regarded as a Tube-MPC system subject to a reduced residual disturbance $\upsilon(k)$, namely

$$\boldsymbol{x}(k+1) = \boldsymbol{A}(\boldsymbol{\theta})\boldsymbol{x}(k) + \boldsymbol{B}(\boldsymbol{\theta})\boldsymbol{u}_{MPC} + \upsilon(k) \tag{25}$$

In Tube-MPC, the ESO-estimated state is used as the initial condition for prediction, which is given by $\hat{\boldsymbol{x}}(k) = \boldsymbol{x}(k) - \boldsymbol{e}_{ESO,x}(k)$, where $\boldsymbol{e}_x(k)$ denotes the state estimation error. Thus, the prediction error can be written as $\bar{\boldsymbol{e}}_x(k) = \boldsymbol{e}_{ESO,x}(k)$.

According to the stability analysis of the ESO, $\boldsymbol{e}_{ESO,x}(k)$ is bounded. In the error analysis of Tube-MPC, the estimation error can therefore be treated as an additional disturbance. Accordingly, the total disturbance faced by Tube-MPC can be expressed as

$$\upsilon_{tatal}(k)=\upsilon(k)+\upsilon_{ESO,x}(k) \tag{26}$$

where $\upsilon_{ESO,x}(k)$ denotes the equivalent disturbance, and $\left\|\upsilon_{ESO,x}(k)\right\|\le c\left\|e_{ESO,x}(k)\right\|$ is bounded. Therefore, there exists a constant such that

$$e_x(k+1)=\left(A(\theta)+B(\theta)K\right)e_x(k)+\upsilon_{tatal}(k) \tag{27}$$

where K is the feedback gain matrix designed for Tube-MPC.

For any disturbance satisfying $\left\|\upsilon_{tatal}(k)\right\|\le\bar{\upsilon}_{tatal}$, there exist $P_{tube}>0$, $\alpha_{tube}>0$, and $\sigma_{tube}>0$, such that

$$V_{tube}\left(e_x(k+1)\right)-V_{tube}\left(e_x(k)\right)\le-\alpha_{tube}\left\|e_x(k)\right\|^2+\sigma_{tube}\left\|\upsilon_{tatal}(k)\right\|^2 \tag{28}$$

On the other hand, from the Lyapunov inequality of the ESO, it follows that

$$V_o\left(e_E(k+1)\right)-V_o\left(e_E(k)\right)\le-\alpha_o\left\|e_E(k)\right\|^2 \tag{29}$$

where $\alpha_o>0$.Based on the above analysis, the following Lyapunov function is constructed:

$$V_{total}(k)=V_{tube}(k+1)-\lambda V_o\left(e_E(k)\right) \tag{30}$$

where $\lambda>0$ is a weighting coefficient to be determined. Then,

$$\begin{aligned}V_{total}(k+1)-V_{total}(k)&=\left[V_{tube}\left(e_x(k+1)\right)-V_{tube}\left(e_x(k)\right)\right]-\lambda\left[V_o\left(e_E(k+1)\right)-V_o\left(e_E(k)\right)\right]\\&\le-\alpha_{tube}\left\|e_x(k)\right\|^2+\sigma_{tube}\left\|\upsilon_{tatal}(k)\right\|^2-\lambda\alpha_o\left\|e_E(k)\right\|^2\end{aligned} \tag{31}$$

Using the boundedness of the disturbance, one obtains

$$V_{total}(k+1)-V_{total}(k)\le-\alpha_{tube}\left\|e_x(k)\right\|^2+\sigma_{tube}\bar{\upsilon}_{tatal}-\lambda\alpha_o\left\|e_E(k)\right\|^2 \tag{32}$$

Therefore, when the external disturbance $\Phi(k)$ is bounded and sufficiently small, an appropriate λcan be selected such that the influence of the disturbance term on the right-hand side is arbitrarily small. Consequently, in the absence of external disturbances, one has

$$V_{total}(k+1)-V_{total}(k)\le-c\left\|\left(e_x(k),e_E(k)\right)\right\|^2 \tag{33}$$

which indicates that the closed-loop origin is asymptotically stable. When bounded disturbances exist, $\left(e_x(k),e_E(k)\right)$ remains bounded and eventually converges to a compact set in a neighborhood of the origin.

3. Results

The proposed ETMPC with an adaptive prediction horizon N_p is validated through comparative simulations. The simulation condition is set as $H=5km$ and $Ma=0.35$. The constrained variables are the turbine inlet temperature $T_4\le1600K$ and the low-pressure compressor surge margin $SMF\ge15$. The total simulation time is 10 s. At $t=0s$, the engine controlled variables are the low-pressure rotor speed $N_1=10000$ and high-pressure rotor speed $N_2=34630$, n rpm. At $t=3s$, an acceleration process is simulated, and the desired terminal values are set as $N_1=13000$ and $N_2=40700$. To simulate uncertainty disturbances, 2% random parameter perturbations ΔA and ΔB are added throughout the simulation based on $B(\theta)$. In addition, a sinusoidal external disturbance with an amplitude of 1% of the rotational speed is introduced during 6–8 s.

To quantitatively evaluate the control performance, three indicators are considered: rise time, disturbance-induced peak deviation, and constraint satisfaction. The rise time is used to assess the dynamic tracking performance during acceleration, while the peak deviation during 6–8 s is used to evaluate disturbance rejection capability. Constraint satisfaction is verified by checking whether the turbine inlet temperature and low-pressure compressor surge margin remain within their prescribed safety limits throughout the simulation.

As shown in Figure 3 and Figure 4, the fixed-N_p ETMPC, the adaptive-N_p ETMPC, and the

adaptive-N_p ETMPC with ESO compensation can all achieve stable tracking of the high- and low-pressure rotor speeds. Meanwhile, the turbine inlet temperature and the low-pressure compressor surge margin remain within the prescribed safety constraints, indicating that all three control schemes possess basic constraint-handling capability.

From the dynamic response results, compared with the fixed-N_p ETMPC, the adaptive-N_p method reduces the rise time of the low-pressure rotor speed by approximately 29.6%. As shown in Figure 5, the prediction horizon automatically increases during the acceleration and disturbance stages, and gradually decreases when the system approaches steady operation. This indicates that the proposed method can adaptively adjust the prediction range according to the system operating condition, thereby avoiding unnecessary computational burden while maintaining control performance. From the perspective of disturbance rejection, after introducing ESO compensation into the adaptive-N_p ETMPC, the output fluctuations caused by external disturbances are significantly reduced. Compared with the adaptive-N_p ETMPC without ESO, the disturbance peaks of N_1 and N_2 are reduced by approximately 88.1% and 80.5%, respectively.

Overall, the adaptive prediction horizon mainly improves the dynamic response during the acceleration stage, while ESO compensation mainly enhances the output stability under disturbances. The combination of the two enables a favorable balance among tracking performance, constraint safety, and disturbance rejection robustness.

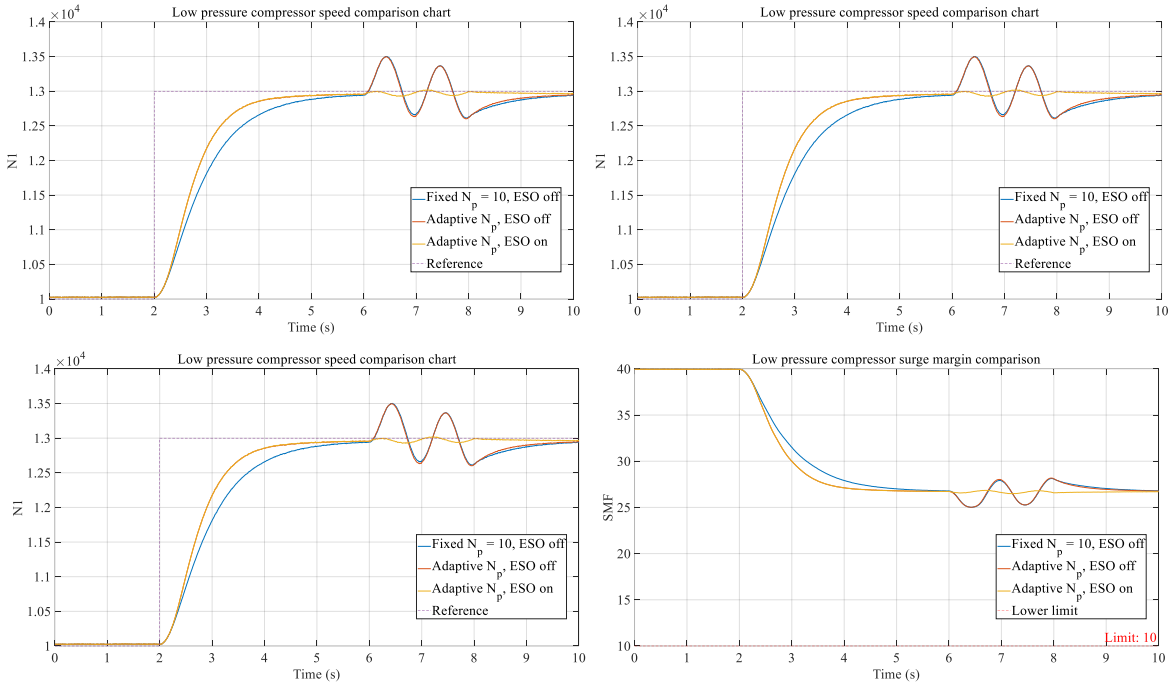


Figure 3. Comparison of Aircraft Engine Output

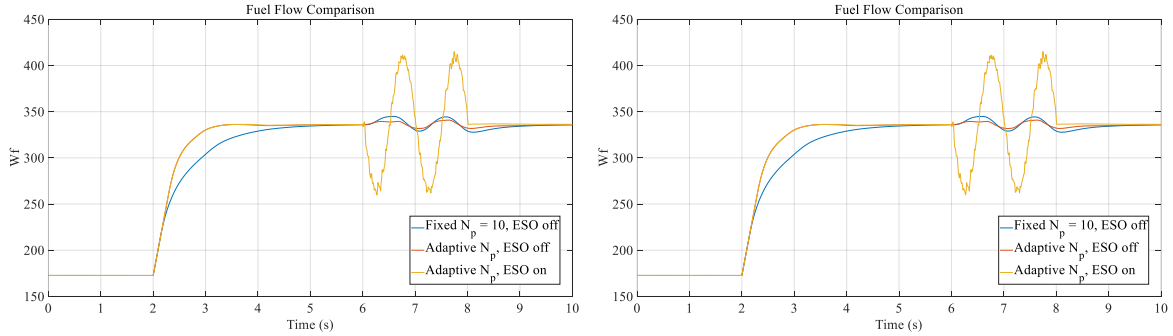


Figure 4. Comparison of Aircraft Engine Control Parameters

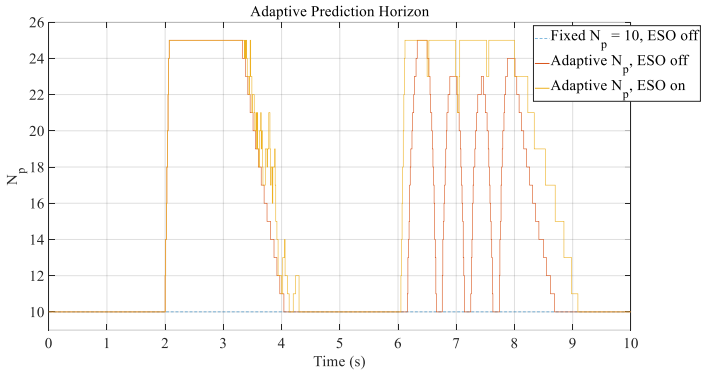


Figure 5. Comparison of adaptive prediction horizons

4. Disscusions

The proposed robust ETMPC with an adaptive prediction horizon can achieve stable tracking of aero-engine rotational speed under model parameter perturbations and external disturbances, while ensuring that key safety variables remain within their prescribed constraints. This demonstrates the favorable constraint-handling capability and disturbance rejection robustness of the proposed method. By introducing the adaptive prediction horizon mechanism, the controller can dynamically adjust the prediction length according to the state deviation and disturbance intensity. Specifically, the prediction horizon is increased during acceleration to improve the anticipation of future state variations and constraint risks, and reduced when the system approaches steady operation to avoid unnecessary computational burden.

Furthermore, by combining ESO-based disturbance estimation with Tube-MPC constraint tightening, the controller can estimate and compensate model uncertainties and external disturbances online, thereby improving constraint safety under disturbed conditions. The integration of the adaptive prediction horizon and ESO-based robust compensation enables a balanced trade-off among tracking accuracy, constraint satisfaction, disturbance rejection, and computational efficiency, providing a feasible solution for real-time robust optimal control of aero-engines during fast dynamic processes.

It should be noted that the present study is mainly based on numerical simulations under a representative flight condition. Although the results verify the effectiveness of the proposed method under parameter perturbations and external disturbances, further validation is still required under broader flight envelopes, actuator saturation, sensor noise, and real-time hardware constraints.

Overall, the proposed method offers a practical framework for real-time robust optimal control of aero-engines. Future work will focus on validation under more complex flight envelopes, actuator dynamic constraints, and hardware-in-the-loop simulation platforms to further improve its engineering applicability.

5. Contact Author Email Address

Linfeng Gou: goulinfeng@nwpu.edu.cn

6. Copyright Statement

The authors confirm that they, and/or their company or organization, hold copyright on all of the original material included in this paper. The authors also confirm that they have obtained permission, from the copyright holder of any third party material included in this paper, to publish it as part of their paper. The authors confirm that they give permission, or have obtained permission from the copyright holder of this paper, for the publication and distribution of this paper as part of the ICAS proceedings or as individual off-prints from the proceedings.

References

[1] Zhang X, Wang Z, Xiao B, and Ye Y A Neural Network Learning-Based Global Optimization Approach for Aero-Engine Transient Control Schedule, *Neurocomputing*, Vol. 469, 2022, pp. 180–188.

[2] Litt JS, Kratz JL, Bianco SJ, Sachs-Wetstone JJ, Dever TP, Buescher HE, Ogden NC, Valdez FD, Budolak DW, Boucher MJ, Patterson AP, and Jansen RH Control Architecture for a Concept Aircraft with a Series/Parallel Partial Hybrid Powertrain and Distributed Electric Propulsion, presented at the AIAA SciTech Forum, 2023.

[3] Sun R-Q, Han X-B, Chen Y-X, and Gou L-F Hyperelliptic Kalman Filter-Based Aeroengine Sensor Fault FDIA System under Multi-Source Uncertainty, *Aerospace Science and Technology*, Vol. 132, 2023, p. 108058.

[4] Zhao Y, Chen C, Xu C, Du X, Huang D, Tsoutsanis E, and Cen Z H_{infty} Rate Bumpless Transfer Control for Aero-Engine Control Systems via Switched Affine Models, *IEEE/ASME Transactions on Mechatronics*, Vol. 30, No. 6, 2025, pp. 7832–7842.

[5] Lv C, Chang J, Bao W, and Yu D Recent Research Progress on Airbreathing Aero-Engine Control Algorithm, *Propulsion and Power Research*, Vol. 11, No. 1, 2022, pp. 1–57.

[6] Montazeri-Gh M, Rasti A, Jafari A, and Ehteshami M Design and Implementation of MPC for Turbofan Engine Control System, *Aerospace Science and Technology*, Vol. 92, 2019, pp. 99–113.

[7] Hou G, Gong L, Huang C, and Zhang J Fuzzy Modeling and Fast Model Predictive Control of Gas Turbine System, *Energy*, Vol. 200, 2020, p. 117465.

[8] Wang P-B, Ren X-M, and Zheng D-D Robust Nonlinear MPC With Variable Prediction Horizon: An Adaptive Event-Triggered Approach, *IEEE Transactions on Automatic Control*, Vol. 68, No. 6, 2023, pp. 3806–3813.

[9] Girard A Dynamic Triggering Mechanisms for Event-Triggered Control, *IEEE Transactions on Automatic Control*, Vol. 60, No. 7, 2015, pp. 1992–1997.

[10] Li P, Kang Y, Wang T, and Zhao Y-B Disturbance Prediction-Based Adaptive Event-Triggered Model Predictive Control for Perturbed Nonlinear Systems, *IEEE Transactions on Automatic Control*, Vol. 68, No. 4, 2023, pp. 2422–2429.

[11] Yan Z, Le X, and Wang J Tube-Based Robust Model Predictive Control of Nonlinear Systems via Collective Neurodynamic Optimization, *IEEE Transactions on Industrial Electronics*, Vol. 63, No. 7, 2016, pp. 4377–4386.

[12] Wang T, Kang Y, Li P, Zhao Y-B, and Yu P Robust Model Predictive Control for Constrained Networked Nonlinear Systems: An Approximation-Based Approach, *Neurocomputing*, Vol. 418, 2020, pp. 56–65.

[13] Zhang Y, Edwards C, Belmont M, and Li G Robust Model Predictive Control for Constrained Linear System Based on a Sliding Mode Disturbance Observer, *Automatica*, Vol. 154, 2023, p. 111101.

[14] Kong L, and Yuan J Disturbance-Observer-Based Fuzzy Model Predictive Control for Nonlinear Processes with Disturbances and Input Constraints, *ISA Transactions*, Vol. 90, 2019, pp. 74–88.

[15] Song P, Yang Q, Li D, Wen G, Zhang Z, and Peng J Disturbance-Compensation-Based Predictive Sliding Mode Control for Aero-Engine Networked Systems With Multiple Uncertainties, *IEEE Transactions on Automation Science and Engineering*, Vol. 22, 2025, pp. 276–292.